

MODELING THE FLOW OF AQUEOUS HUMOR IN POSTERIOR CHAMBER

Ram Avtar, Swati Srivastava¹

Department of Mathematics, Harcourt Butler Technological Institute, Kanpur 208002, India

¹Corresponding Author e-mail: feb13swati@gmail.com

Abstract

A simple mathematical model for the aqueous flow in the posterior chamber (iris-lens channel) of the anterior segment of the eye is developed for an analysis of the aqueous humor fluid dynamics in the posterior chamber. The aqueous humor is treated as a viscous (Newtonian), incompressible, homogeneous, isotropic fluid with creeping flow. The iris-lens channel formed from the space between concentric spherical shell segments is modeled as a spherical disc-shaped region conforming to the lens curvature with a variable channel height. An analytical solution of the model is obtained. The computational results for pressure, fluid velocity and stress distributions are presented through graphs and the effects of model parameters on the velocity and stresses are illustrated and discussed.

Keywords: Aqueous humor, iris-lens channel, posterior chamber.

INTRODUCTION

The aqueous humor fluid secreted by the ciliary epithelium in the rear (posterior) chamber, behind the iris flows through the pupil into the front (anterior) chamber. It drains through the trabecular meshwork/ canal of Schlemm into the episcleral venous system. The circulation of aqueous humor in the anterior segment of the eye is necessary for maintaining the IOP and inflation of the eye globe, the nutritional supply to the avascular ocular tissue: posterior cornea, trabecular meshwork, lens and anterior vitreous and for providing transparent medium/refractive medium in the eye. Any obstruction to the flow of aqueous humor at any level of the anterior segment may result in some pathological states. Resistance to the aqueous movement from its secretion-site within the posterior chamber through the pupillary aperture produces a pressure gradient across the iris which forces the iris anteriorly in the trabecular meshwork thereby closing the angle which results in primary closed-angle glaucoma.

The aqueous humor occupying the anterior and posterior chambers is divided by the iris which is a ring of muscle fibres. Thus, it is an elastic solid membrane. The aqueous humor flows from the posterior chamber to the anterior chamber through the pupil. To ensure this forward flow of aqueous humor the fluid pressure in the posterior chamber must be higher than that in the anterior chamber, pushing the iris anteriorly. The fluid pressure in the anterior chamber which is higher than that in the posterior chamber pushes the iris against the lens, preventing backward flow from the anterior chamber into the posterior chamber. Thus, a net force applied on the iris by the higher fluid pressure in the anterior chamber displaces the iris posteriorly and it assumes a concave shape.

The flexible position of iris which is dependent on the pressure differential across it influences the flow of aqueous humor in the posterior chamber. Under some pathological conditions, the iris assumes convex shape which may contribute to the development of closed-angle glaucoma, whereas under some other pathological /abnormal conditions, the iris takes on the concave shape which may contribute to the development of pupillary-block glaucoma. Experimental investigations as well as theoretical studies are required to examine how the position of elastic iris influences the aqueous humor fluid dynamics in the posterior chamber and how certain forms of glaucoma are associated with the displacement of iris from its normal contour.

Friedland (1978) developed the first hydrodynamic model of aqueous humor in the posterior chamber by assuming it as a spherical segment incorporated into a synthesized electric current analog of flow between ciliary artery and episcleral vein. Tiedeman (1991) proposed a model for the contour of the iris by assuming it as a pressure relief valve with a conclusion that the forward curvature of the iris increases with more interior lens position and with a mid-dilated pupil. Heys et al. (2001) developed a two-dimensional mathematical model of the coupled aqueous humor system, solved by FEM and simulate that the iris is displaced by the aqueous humor as it circulates through the anterior segment. They also modeled the blinking process by applying a normal stress along the cornea. Heys and Barocas (2002) presented a mathematical model of the coupled aqueous humor-iris system to predict the effects of the iris accommodation on the iris position and pressure distribution in the aqueous humor. Huang and Barocas (2004) tried to explore the steady-state simulations of the coupled fluid-solid system and predicted that maximum pupillary block and angle closure occur at the minimum pupil dilation. Avtar and Srivastava (2009) proposed a simple mathematical model concerned with the study of fluid dynamics of aqueous humor in the posterior chamber under normal and some pathological states.

The present paper is devoted to the development of a simple mathematical model for the flow of aqueous humor in the posterior chamber i.e. iris-lens channel treated as a sector of sphere. The lens is treated as fixed and the iris as elastic solid flexible membrane, the position of which depends on the pressure differential across it. The model is solved analytically and the results for the fluid pressure, velocity and stress distributions are computed and presented through graphs. The sensitivity of the flow characteristics to the model parameters is illustrated and discussed.

MATHEMATICAL FORMULATION

The posterior chamber is the fluid-filled space bounded by the back of the iris and the front surface of the lens. The posterior surface of the iris and anterior surface of lens-zonule-vitreous are assumed to form two concentric spherically-capped anterior and posterior borders of the, taken in the shape of a sector of a sphere of the iris-lens channel of radii of curvature $(R+h)$ and R , respectively at the pupil margin. The posterior chamber is considered axisymmetric with respect to the pupillary axis. It is assumed that the pupil subtends angle θ_p with respect to the pupillary axis and the ciliary body θ_{CB} .

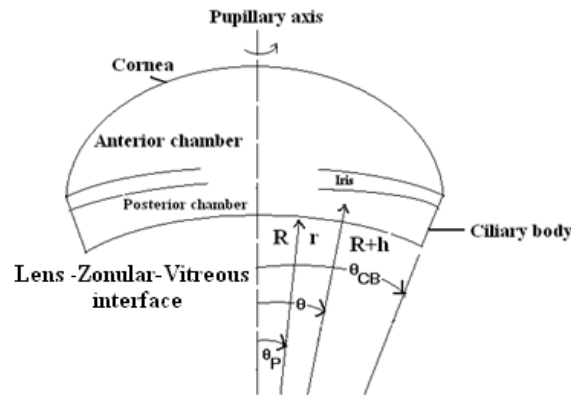


Fig. 1. Schematic model for the posterior chamber [Friedland, 1978]

The iris is represented by an incompressible linear elastic solid flexible membrane that deforms in proportion to the local pressure drop across it. The lens is assumed to be rigid. The height between the iris and lens is described as:

$$h = h_0 \left[1 + \left(\frac{P(\theta) - P_I}{E} \right) \right],$$

where E is the elastic modulus of the iris, h_0 is the undeformed height between the iris-lens channel, P_I is the intraocular pressure and $P(\theta)$ is the fluid pressure in the posterior chamber.

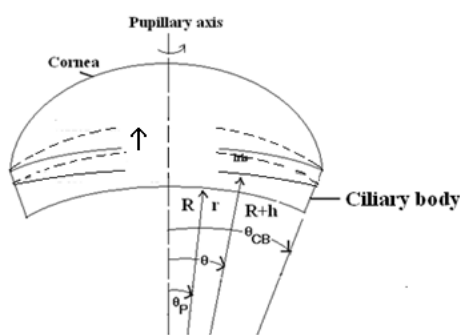


Fig. 2(a) Upward movement of iris when

$$P_i < P(\theta), \text{ abnormally}$$

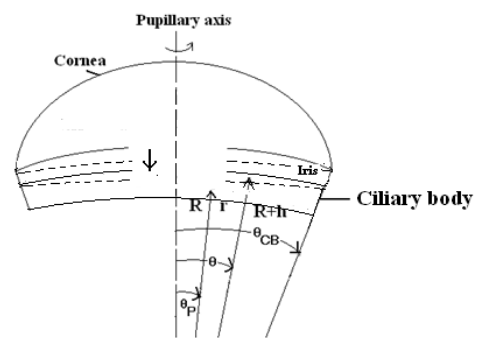


Fig. 2(b) Downward movement of

$$P_i > P(\theta)$$

Governing Equations

The aqueous humor is treated as an incompressible fluid of constant density and viscosity. The equations which govern the fluid flow are the Navier-Stokes equations and the continuity equation given below:

$$\rho \frac{d\bar{V}(r, \theta, \phi)}{dt} = -\bar{\nabla}P(r, \theta, \phi) + \mu \nabla^2 \bar{V}(r, \theta, \phi) \quad (1)$$

where $\bar{V}(r, \theta, \phi) = V_r \bar{e}_r + V_\theta \bar{e}_\theta + V_\phi \bar{e}_\phi$, V_r, V_θ, V_ϕ , and $P(r, \theta, \phi)$ are the fluid velocity components and fluid pressure, respectively. The symbols t, ρ and μ are the time, fluid density, and viscosity, respectively. For an incompressible fluid, the equation of continuity is specified as:

$$\bar{\nabla} \cdot \bar{V}(r, \theta, \phi) = 0. \quad (2)$$

Since the channel has been taken to be symmetric with respect to the azimuthal angle ϕ , the flow dynamics are also assumed to be independent of ϕ . The imposition of symmetry condition simplifies our model causing both \bar{V} and P to be independent of ϕ within the iris-lens channel. The continuity equation assumes the form:

$$\frac{\partial \bar{V}(r, \theta, \phi)}{\partial \theta} + \bar{V}(r, \theta, \phi) \cot \theta = 0. \quad (3)$$

The solution to the continuity equation (3) can be written in the following form:

$$\bar{V}(r, \theta, \phi) = V_\theta(r, \theta) \bar{\varepsilon}_\theta = \frac{\alpha v_\theta(r)}{\sin \theta} \bar{\varepsilon}_\theta, \quad (4)$$

where $V_\theta(r, \theta)$ is the magnitude of the flow velocity in the θ direction as a function of both r and θ , α is a constant, $v_\theta(r)$ is the radial component of $V_\theta(r, \theta)$, and $\bar{\varepsilon}_\theta$ is the unit vector in the θ direction.

The flow of aqueous humor in the narrow iris-lens channel with variable passage/height is treated as a steady creeping flow. In view of the axial symmetry, negligible body forces, inertial and non-linear convective acceleration terms and lubrication assumptions, the equation of motion (2) is simplified in the form:

$$0 = -\frac{\partial p}{\partial r} \quad (5)$$

$$0 = -\frac{1}{r} \frac{\partial p}{\partial \theta} + \mu \left[\frac{1}{r^2} \frac{\partial}{\partial r} \left(r^2 \frac{\partial v_\theta}{\partial r} \right) \right] \quad (6)$$

$$0 = -\frac{\partial p}{\partial \phi} \quad (7)$$

Equations (5) and (7) imply that

$$P(r, \theta, \phi) = P(\theta). \quad (8)$$

Substituting equation (4) and (8) into equation (6) we get:

$$\frac{1}{r\mu} \frac{\partial P(\theta)}{\partial \theta} = \frac{\alpha}{\sin \theta} \left[\frac{\partial^2 v_\theta(r)}{\partial r^2} + \frac{2}{r} \frac{\partial v_\theta(r)}{\partial r} \right]. \quad (9)$$

Separating it into r and θ we have,

$$\sin \theta \frac{dP}{d\theta} = B \quad (10i)$$

$$\frac{\mu}{r} \frac{d}{dr} \left(r^2 \frac{dv_\theta(r)}{dr} \right) = B, \quad (10ii)$$

where B is a constant.

Boundary Conditions:

For complete specification of the mathematical model, appropriate boundary conditions must be imposed. Physically realistic and mathematically consistent boundary conditions are prescribed as follows:

$$(i) \quad P = P(\theta_p) \quad \text{at } \theta = \theta_p, \quad (11)$$

$$(ii) \quad P = P(\theta_{CB}) \quad \text{at } \theta = \theta_{CB}. \quad (12)$$

Along the walls of the iris-lens channel no-slip boundary conditions are prescribed as:

$$(iii) \quad v_\theta(R) = v_\theta(R+h) = 0, \quad (13)$$

where $P(\theta_p)$ and $P(\theta_{CB})$ are the pressures at θ_p and θ_{CB} respectively.

Solution to the Model:

Equation (10i) yields,

$$P(\theta) = B \ln \tan(\theta / 2) + C_1, \quad (14)$$

where C_1 is an integration constant. Subjecting this solution to the boundary conditions (11) and (12), the expression for fluid pressure is obtained in the form:

$$P(\theta) = \frac{1}{\ln \left(\frac{\tan(\theta_p / 2)}{\tan(\theta_{CB} / 2)} \right)} \left[P(\theta_p) \ln \left(\frac{\tan(\theta / 2)}{\tan(\theta_{CB} / 2)} \right) + P(\theta_{CB}) \ln \left(\frac{\tan(\theta_p / 2)}{\tan(\theta / 2)} \right) \right]. \quad (15)$$

Solving equation (10ii), in conjunction with equation (4) and subject to the boundary conditions in equation (13), gave the following expression for the flow velocity:

$$V_{\theta}(r, \theta) = \frac{-[P(\theta_{CB}) - P(\theta_p)][(2R + h) - r - R(R + h) / r]}{2\mu \sin \theta \ln[\tan(\theta_{CB} / 2) / \tan(\theta_p / 2)]}. \quad (16)$$

The Navier-Stokes equations for the fluid flow velocities have been defined/used with respect to a standard spherical coordinate system where increasing θ is opposite to the flow direction. Therefore, minus sign occurs in the right hand side of the equation (16). Thus, the minus sign signifies the direction of flow toward the pupil.

The normal stress at the iris wall of the posterior chamber for an incompressible fluid is given by:

$$\tau_{\theta\theta} = -\mu \left[2 \left(\frac{1}{r} \frac{\partial V_{\theta}}{\partial \theta} + \frac{V_r}{r} \right) \right],$$

$$\therefore \tau_{\theta\theta} = -\frac{1}{r} \frac{\cos \theta}{\sin^2 \theta} \frac{[P(\theta_{CB}) - P(\theta_p)][(2R + h) - r - R(R + h) / r]}{\ln[\tan(\theta_{CB} / 2) / \tan(\theta_p / 2)]}. \quad (17)$$

The shear stress at the iris wall of the posterior chamber is given by:

$$\tau_{r\theta} = -\mu \left[r \frac{\partial}{\partial r} \left(\frac{V_{\theta}}{r} \right) + \frac{1}{r} \frac{\partial V_r}{\partial \theta} \right],$$

$$\therefore \tau_{r\theta} = -\frac{r[P(\theta_{CB}) - P(\theta_p)]}{2 \sin \theta \ln[\tan(\theta_{CB} / 2) / \tan(\theta_p / 2)]} \left[(2R + h) \ln r + 2R(R + h) / r^3 \right]. \quad (18)$$

RESULTS AND DISCUSSIONS

The computational results for the fluid pressure, velocity and the stress distributions are obtained using the values of model parameters given in the following table and presented through graphs. Also the effects of various parameters on these are illustrated.

Table 1. Parameters appearing in the model and their estimated subsequent values in the posterior chamber:

Parameter	Description	Typical physiological value*
R	Radius of curvature	1 mm
μ	Viscosity of aqueous humor	0.008 gm/(cm sec)
$P(\theta_p)$	Pressure at pupillary angle	24 mm Hg
$P(\theta_{CB})$	Pressure at ciliary body angle	30 mm Hg
θ_p	Pupillary angle	15°
θ_{CB}	Ciliary body angle	55°
P_i	Intraocular pressure	20 mm Hg
E	Elastic modulus of iris	9×10^4 dynes / sq.cm
h_0	Height of channel	5 μ m

*Estimated and used by Heys et al.[2001].

The aqueous humor fluid pressure profile in the iris-lens channel has been depicted in fig. 3. The pressure is maximum at the ciliary body angle and it decreases along the channel toward the pupil.

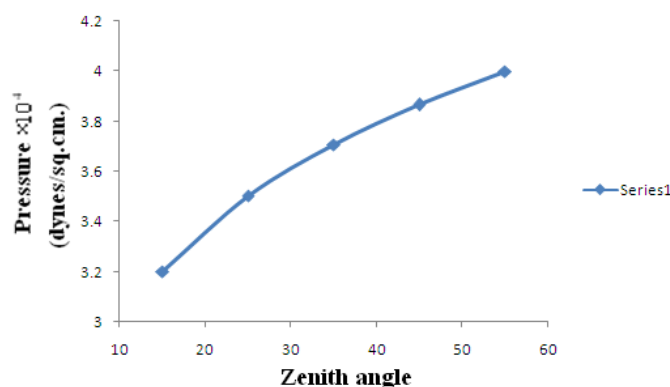


Fig. 3. Fluid-pressure distribution along iris-lens channel

Case I- When the fluid pressure in posterior chamber is higher than that in the anterior chamber, the iris is pushed anteriorly by aqueous humor and assumes convex shape i.e. $P_i < P(\theta)$:

The curves in fig. 4 characterize the fluid-velocity distribution along the iris-lens channel at three different radial positions. The velocity decreases along the channel toward the ciliary body angle. The velocity increases along the radial distance.

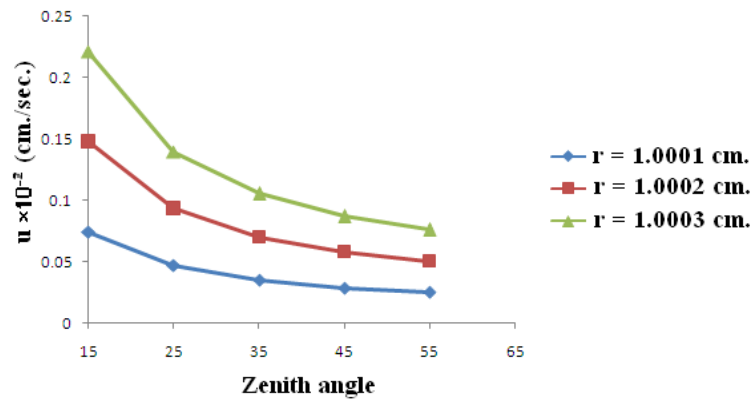


Fig. 4. Fluid velocity distribution along iris-lens channel

The effect of the elastic modulus of the iris on the velocity has been displayed in fig. 5. An increase in the elastic modulus decreases the fluid velocity.

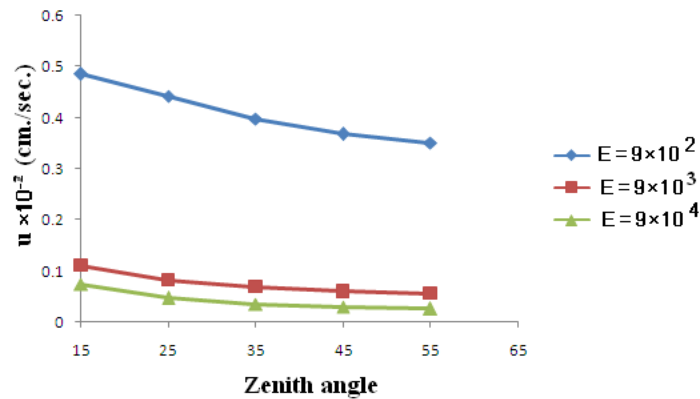


Fig. 5. Effect of elastic modulus on fluid velocity

The effect of the intraocular pressure on the normal stress distribution along the iris-lens channel has been portrayed in fig.6. A rising intraocular pressure decreases the normal stress.

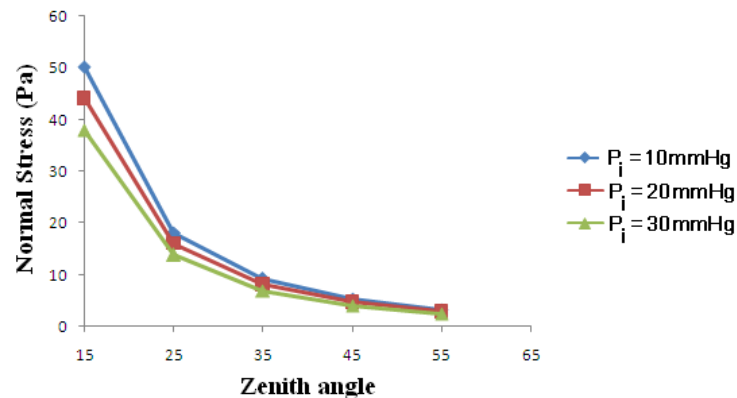


Fig. 6. Effect of intraocular pressure on normal stress

It is observed from fig. 7 that an increase in the elastic modulus reduces the normal stress.

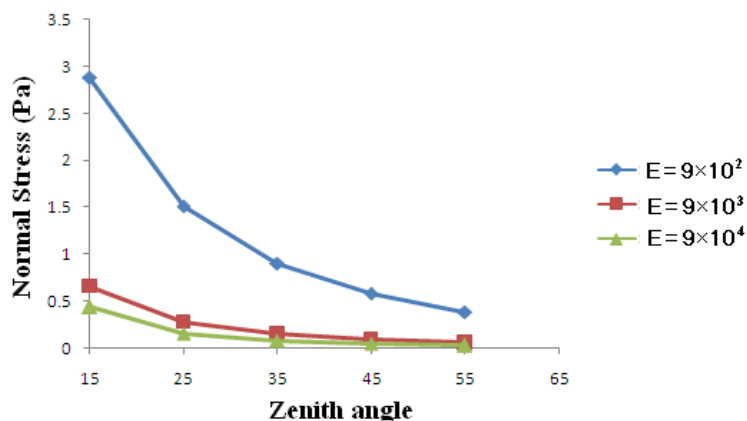


Fig. 7. Effect of elastic modulus on normal stress

The effect of the elastic modulus on the shear stress distribution has been illustrated in fig. 8. The shear stress is decreased with an increase in the elastic modulus.

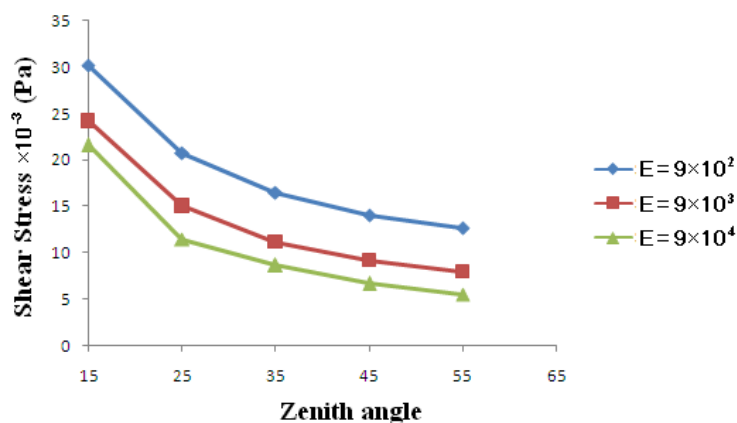


Fig. 8. Effect of elastic modulus on shear stress

Case II- When the fluid pressure in anterior chamber is higher than that in the posterior chamber, the iris is displaced posteriorly towards lens and assumes concave shape i.e. $P_i > P(\theta)$:

It is evident from the curves in fig. 9 that the fluid velocity is minimum at the ciliary body angle and it increases along a direction, opposite to the θ direction. The velocity increases along radial direction. In this case, the flow is slow as compared with that of previous case.

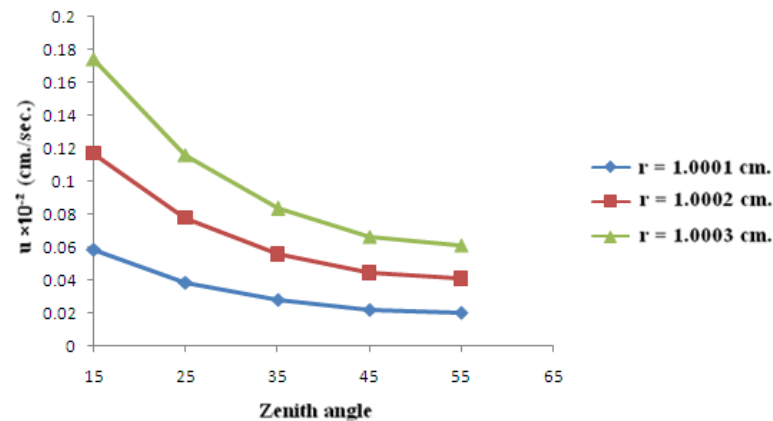


Fig. 9. Fluid velocity distribution along iris-lens channel

The effect of intraocular pressure on the fluid velocity has been shown in fig. 10. A rise in the IOP reduces the velocity as is observed from the graphs.

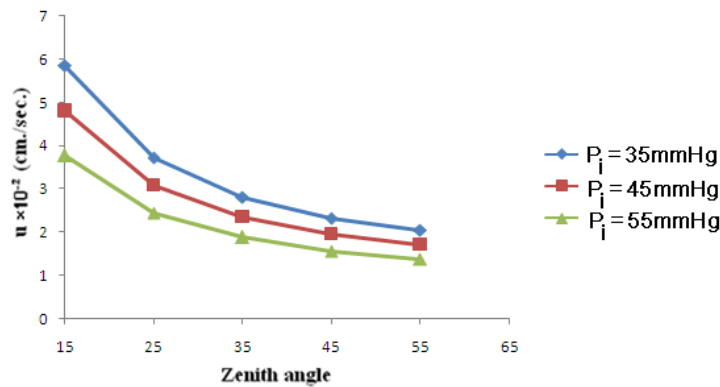


Fig. 10. Effect of intraocular pressure on fluid velocity

It is evident from the graphs in fig. 11 that the flow velocity is decreased with increasing the value of elastic modulus. If $E = 9 \times 10^5$ dynes / sq.cm, the direction of flow is reversed after certain angular distance i.e. the velocity assumes a direction along θ direction.

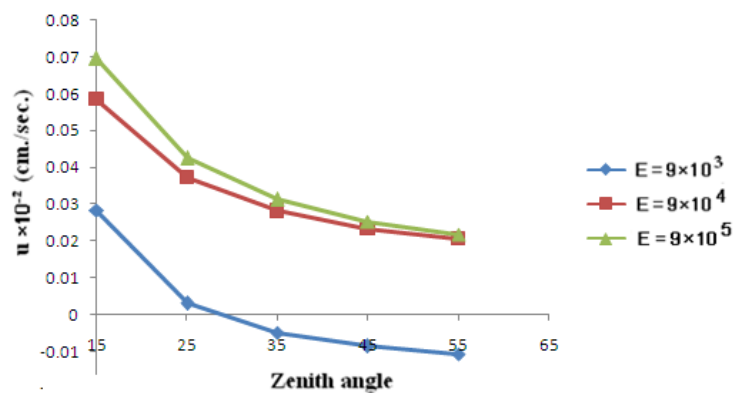


Fig. 11. Effect of elastic modulus on fluid velocity

As is evident from the graphs in fig. 12, the normal stress is reduced with an increase in intraocular pressure.

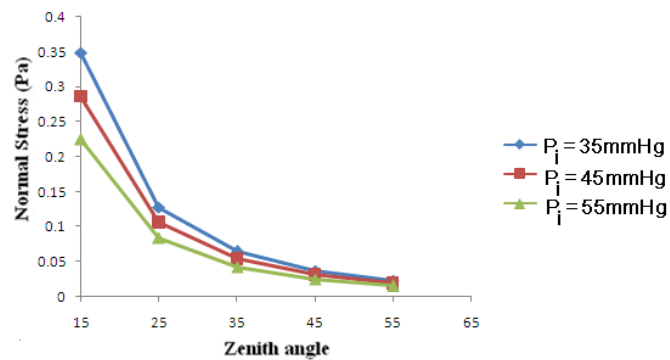


Fig. 12. Effect of intraocular pressure on normal stress

The effect of radial position on the normal stress distribution along the iris-lens channel has been depicted in fig. 13. The normal stress increases along radial distance.

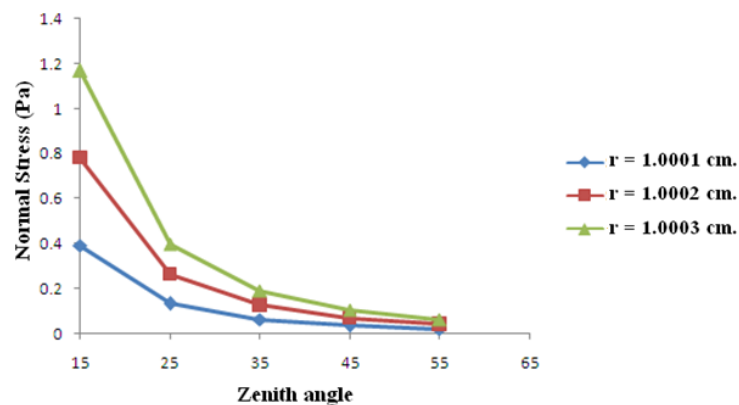


Fig. 13. Effect of r on normal stress

The effect of elastic modulus of the iris on the normal and shear stress distributions along the iris-lens channel has been illustrated in figs. 14 and 15, respectively. As the value of elastic modulus is increased, the values of both normal and shear stresses are increased.

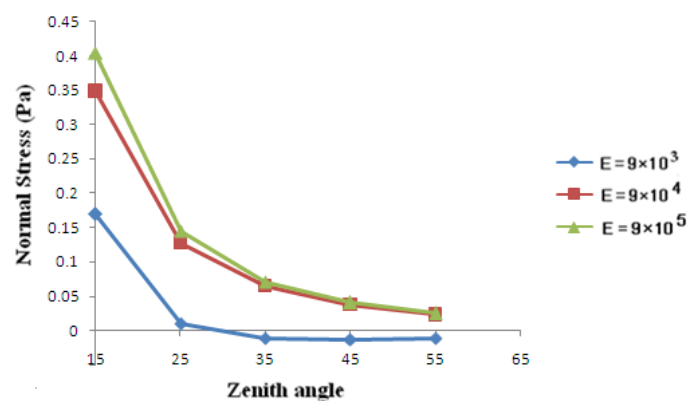


Fig. 14. Effect of elastic modulus on normal stress

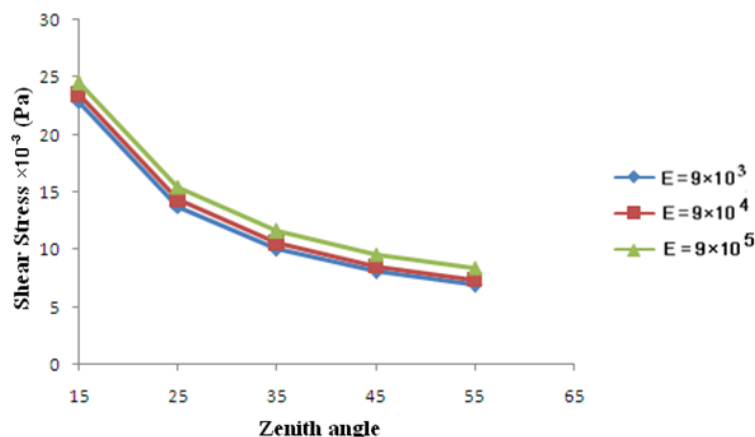


Fig. 15. Effect of elastic modulus on shear stress

CONCLUDING REMARKS

An analysis of the hydrodynamic model for the flow of aqueous humor in the posterior chamber leads to the conclusion that an increase in the elastic modulus of the iris reduces the aqueous flow velocity. A rise in the introduction pressure decreases the fluid velocity and stress. The normal and shear stresses are decreased by an increase in the elastic modulus when the posterior chamber fluid pressure is abnormally higher than the anterior chamber fluid pressure. When the IOP is higher than the fluid pressure in the posterior chamber, both the stresses are increased by an increase in the elastic modulus of the iris.

REFERENCES

- [1] Avtar, R. and Srivastava, R. (2009). "Mathematical model of aqueous humor flow in posterior chamber of the eye". *Int. J. Theor. App. Math.* 4(3), 305-319.
- [2] Heys, J.J. and Barocas, V.H. (2002). "Computational evaluation of the role of accommodation in pigmentary glaucoma". *Invest. Ophthalmol. Vis. Sci.* 43, 700-708.
- [3] Heys, J.J., Barocas, V.H. and Taravella, M.J. (2001). "Modelling passive mechanical interaction between aqueous humor and iris". *J. Bio. Mech. Engg.* 123, 540-547.
- [4] Huang, E.C. and Barocas, V.H. (2004). "Active iris mechanics and pupillary Block: Steady state analysis and comparison with anatomical risk factors". *J. Bio. Med. Engg.* 32(9), 1276- 1285.
- [5] Mapstone, R. (1968). "Mechanics of pupil block" *Br. J. Ophthalmol.* 52, 19-25.
- [6] Tiedeman, J.S. (1991). "A physical analysis of the factors that determine the contour of the Iris" *J. Am. Ophthalmol.* 111, 338-343.
- [7] Friedland, Allan B. (1978). "A hydrodynamic model of aqueous flow in the posterior chamber of the eye" *Bull. Math. Biol.* 40, 223 -235.
- [8] Huang, E.C. and Barocas, V.H. (2006). "Accommodative microfluctuations and iris contour" *J. Vision*, 6, 653-660.